Mechanisms of Aerosol Generation in Liquid-Protected IFE Chambers

M. S. Tillack, A. R. Raffray and M. R. Zaghloul
Center for Energy Research
and Mechanical and Aerospace Engineering Department
Jacobs School of Engineering

US-Japan Workshop on Power Plant Studies
San Diego, CA
9-11 October 2003

Aerosols can interfere with several processes in the target chamber

- Direct-drive target contamination can affect implosion symmetry
- Indirect-drive target contamination can block entrance hole and absorb ion energy
- Laser driver beam can be distorted
- Ion propagation can be affected, depending on transport mode: *∂E/dx*, scattering, stripping, charged droplet effects, ...
- Target trajectory can be perturbed
- In-chamber target tracking can be obscured
- Final optic may become contaminated

Design limits have been developed in ARIES-IFE

Process	**Size limit and basis**	**Density limit and basis**
Direct drive target contamination	50 nm: surface finish degradation	5 mg/m^3 Pb: thickness variation
Indirect drive target contamination		1 g/m^3 Pb (0.3 mg/cm^2): beam absorption on target surface
Target tracking system obscuration	1 μm: position measurement error	10 mg/m^3: tracking & beam absorption
Laser propagation	~0.25 μm: diffraction	~ 1 Torr ($3e^{19}/cm^3$) equivalent: absorption and refraction
Ion propagation:		
Neutralized ballistic transport		Stripping: ~1 mTorr equiv.
Pre-formed channel		Scattering: ~1 Torr equiv.
Self-pinched		Self-pinching process: ~100 mTorr equivalent

A dedicated R&D program is needed to determine values of particle size and density expected to occur in a power plant

Mechanisms of aerosol generation

- Homogeneous nucleation and growth from the vapor phase
  1. Supersaturated vapor
  2. Ion seeded vapor
- Phase decomposition from the liquid phase
  3. Thermally driven phase explosion
  4. Pressure driven fracture
- Hydrodynamic droplet formation (not considered in this talk)

Homogeneous nucleation.
1. Supersaturation drives rapid condensation

$$\Delta G = \frac{4\pi r^3}{3V_m}(\mu_L - \mu_v) + 4\pi\sigma r^2$$

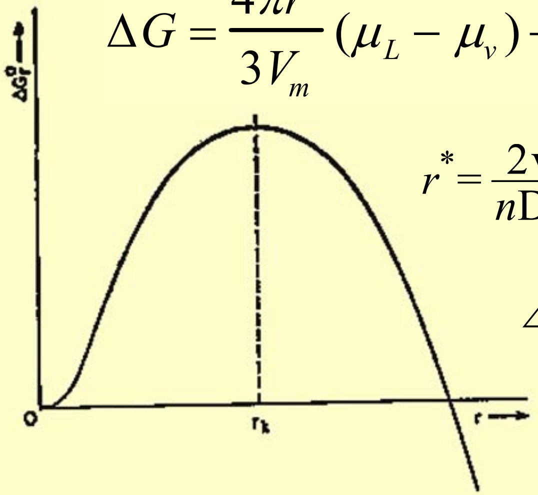

$$r^* = \frac{2\mathrm{v}}{n\mathrm{Dn}}$$

Δμ=k□□□□

$$J_h = Z\,\beta\,C^*$$

$$C^* = \frac{p}{kT}\exp\mathrm{e}- \frac{\mathrm{D}W_k}{kT}\mathrm{c}$$

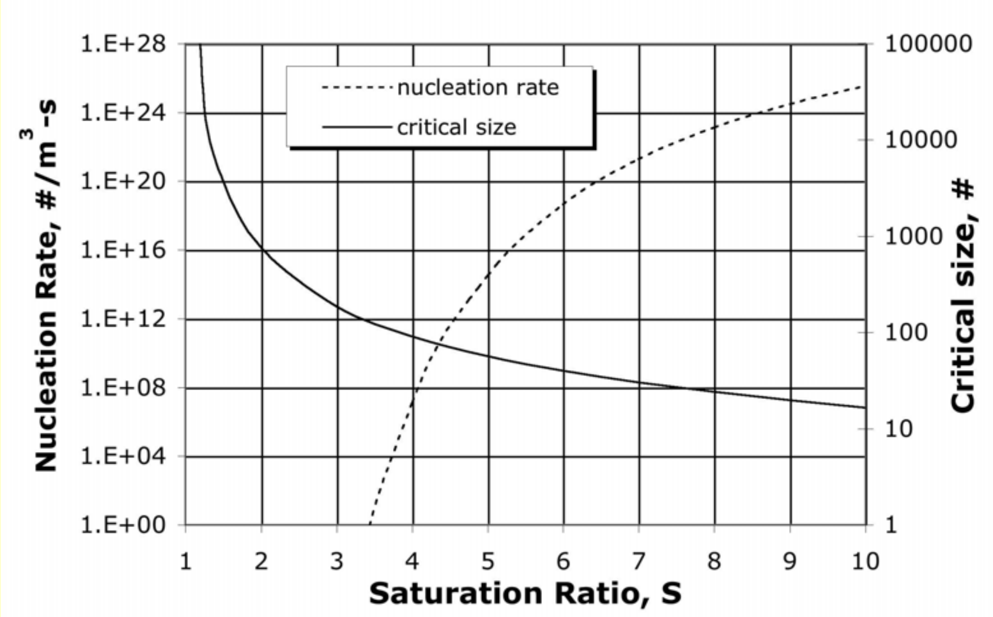

Si, n=10^{20} cm^{-3}, T=2000 K

- **High saturation ratios result from rapid cooling due to plume expansion and heat transfer to the background gas**
- **Very high nucleation rate and small critical radius result**
- **Reduction in S due to condensation shuts down HNR quickly; competition between homogeneous and heterogeneous condensation determines final size and density distribution**

Homogeneous nucleation.
2. Ions enhance the nucleation rate

- **Ion jacketing produces seed sites**
- **Dielectric constant of vapor reduces free energy**

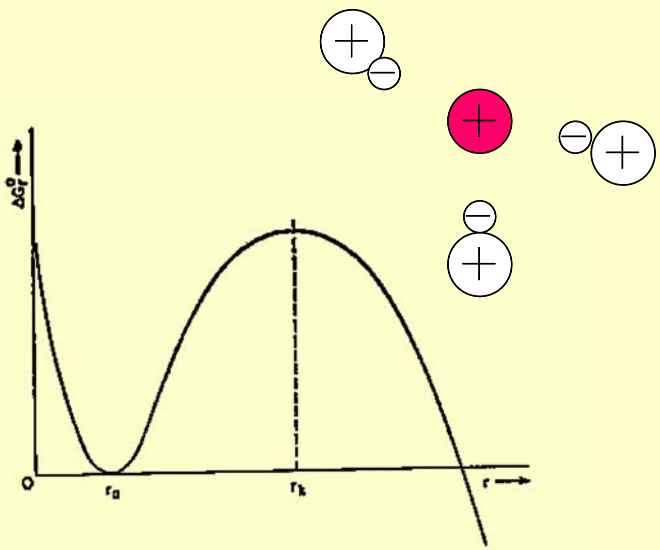

Si, n=10^{20} cm^{-3}, T=2000 K, Z_{eff}=0.01

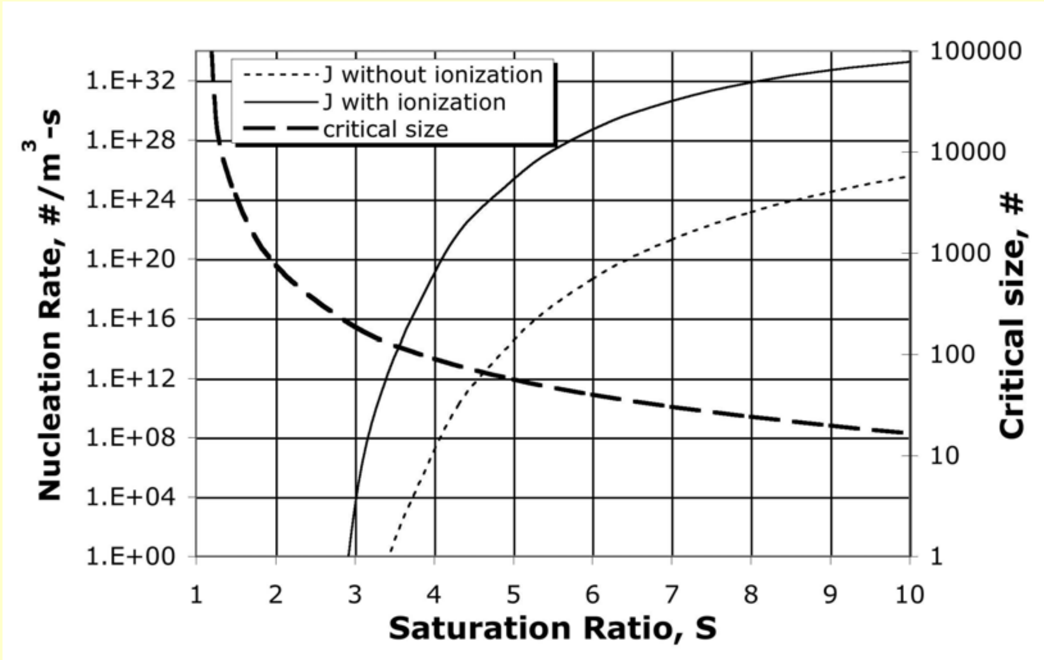

$$\Delta G = \frac{4\pi}{3V_m}(r^3 - r_a^3)(\mu_L - \mu_v) + 4\pi\sigma(r^2 - r_a^2) + \frac{e^2}{2}(1-\varepsilon^{-1})(r^{-1} - r_a^{-1})$$

Mechanisms for phase decomposition: 3. Spinodal decomposition

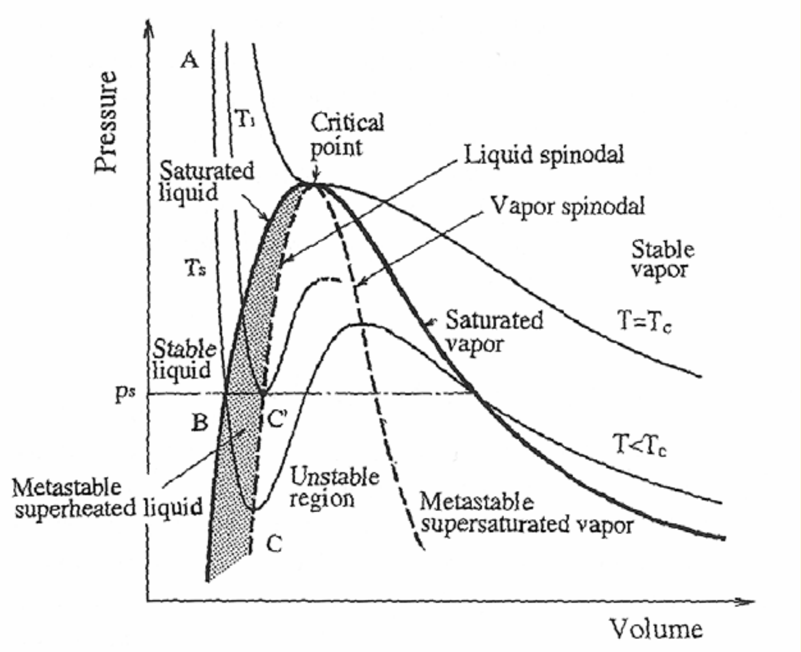

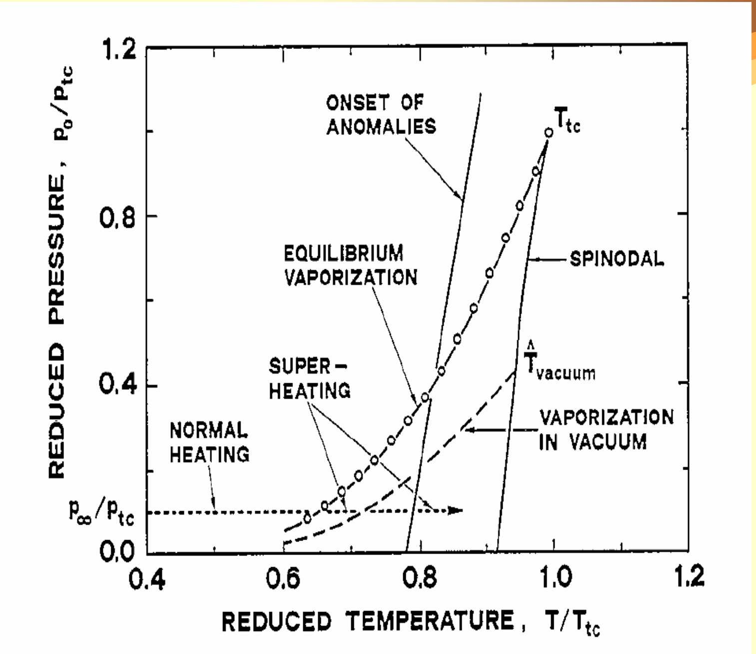

- **Rapid heating (faster than the homogeneous vapor nucleation rate) can drive liquid beyond equilibrium (*superheating*) to a metastable state**
- **The metastable liquid has an excess of free energy, so it decomposes explosively into liquid and vapor phases.**
- **As $T/T_{tc} \rightarrow$ spinodal, Becker-Döhring theory predicts an avalanche-like explosive growth of the nucleation rate (by 20-30 orders of magnitude)**

Disequilibrium alters the free energy equation

The physics of nucleation of *vapor in liquid* is identical to nucleation of *liquid in vapor*

But, for explosive evaporation we need to consider disequilibrium in the pressure balance.

$$W(r) = \frac{4r\, r^3}{3V_m} \_ n_g - n_l i + 4r\, r^2 v - (p_g - p_l)\, V$$

equilibrium: $p_g = p_l + \frac{2v}{r_c}$

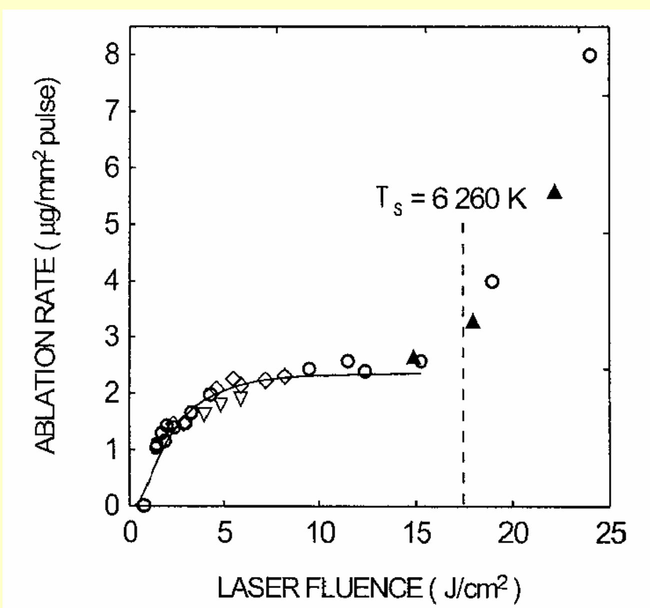

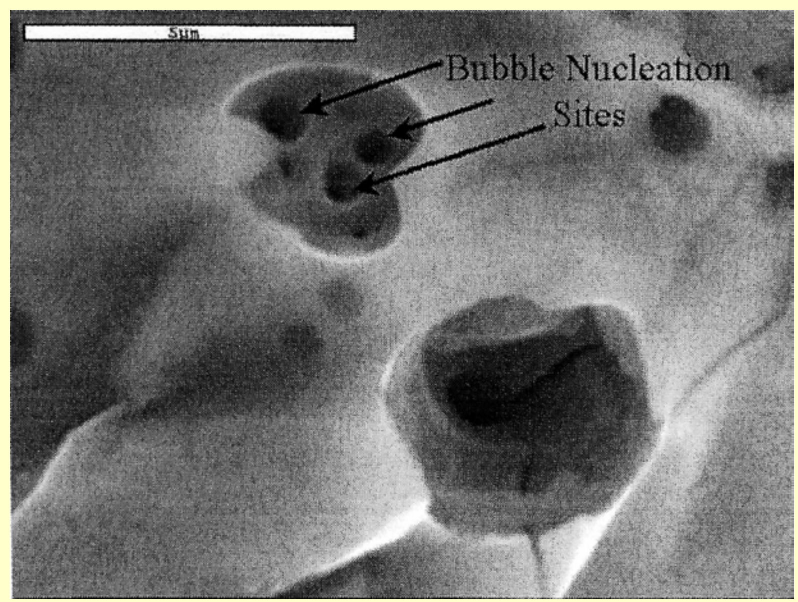

Example: depth of Flibe released, R=6.5

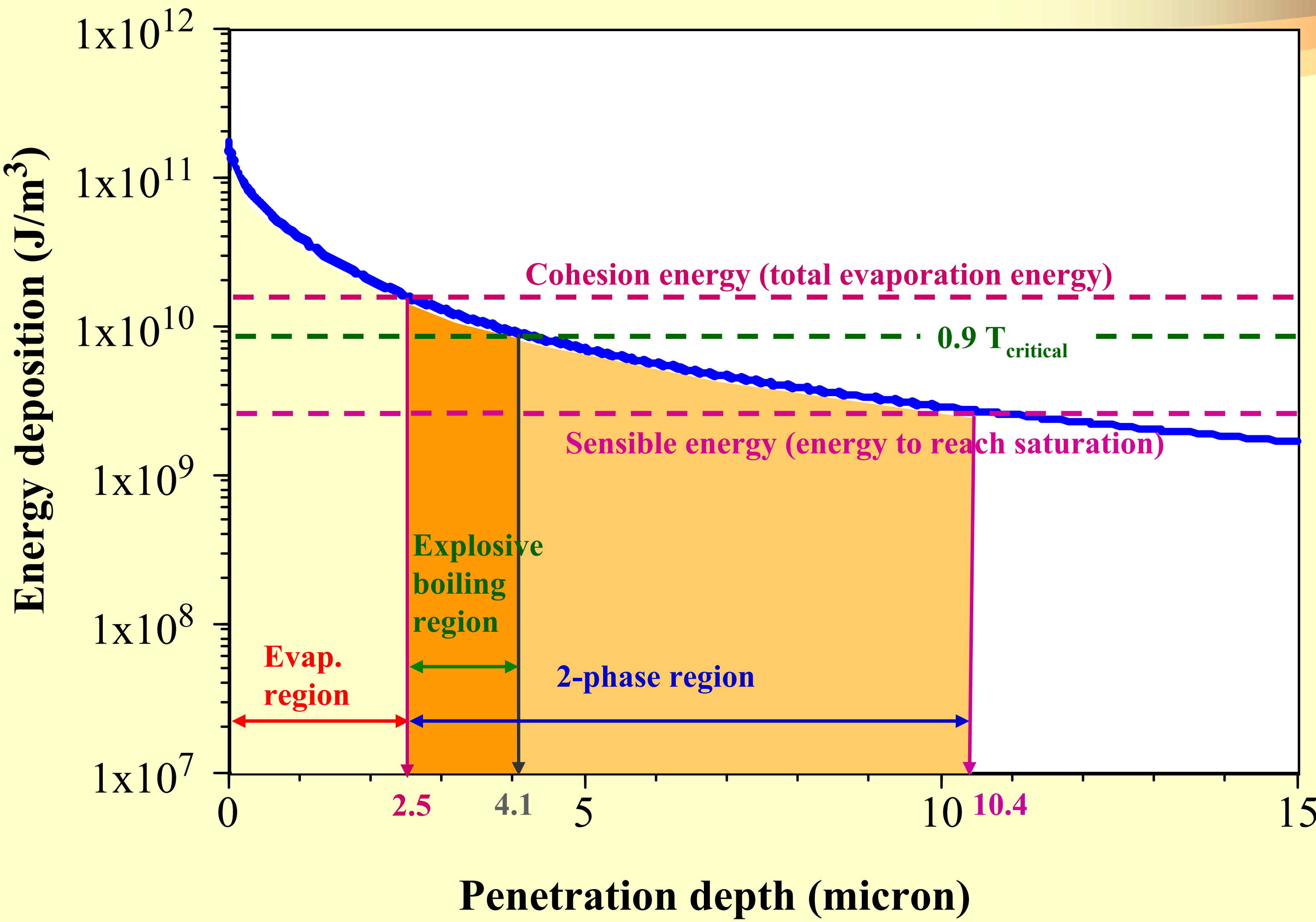

Mechanisms for phase decomposition: 4. Liquid fracture and spalling

3-parameter Morse potential:

$$U(v) = U_{coh}\left[\exp\left(\frac{-2(v-v_0)}{a}\right) - 2\exp\left(\frac{-(v-v_0)}{a}\right)\right]$$

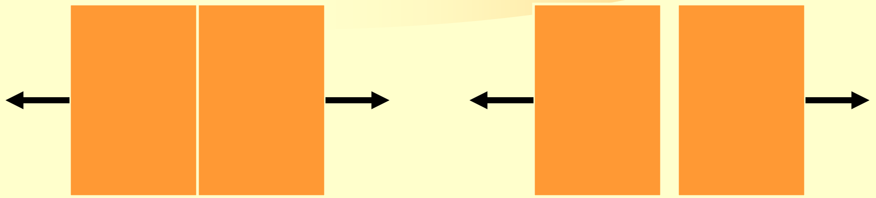

Cold pressure:

$$P(v) = -\frac{dU}{dv} = \frac{2U_{coh}}{a}\left[\exp\left(\frac{-2(v-v_0)}{a}\right) - \exp\left(\frac{-(v-v_0)}{a}\right)\right]$$

Beryllium data

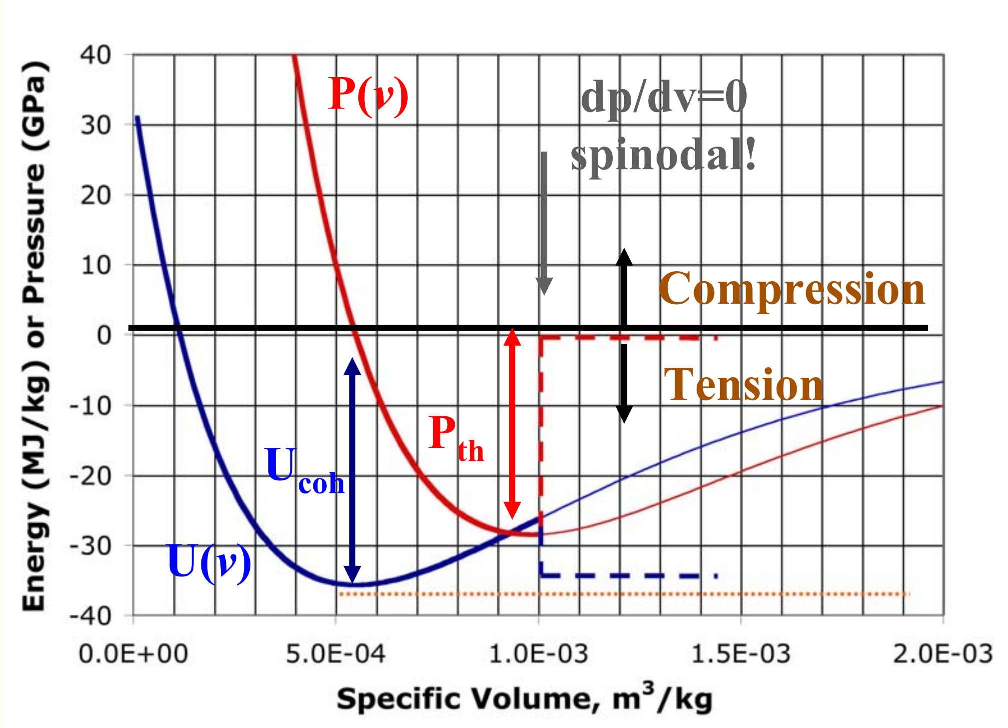

Theoretical spall strength, P_{th}, is given by minimum of P(*v*):

$$P_{th} = \sqrt{\frac{U_{coh} B_0}{8 v_0}}$$

U_{coh} = Specific cohesive energy

$v = 1/\rho$ = Specific volume

v_0 = Specific volume at zero pressure

$a = (2v_0 U_{coh} / B_0)^{1/2}$

B_0 = Bulk modulus

Spalling due to a pressure wave in Flibe reflecting from a perfectly stiff wall@6.5m

$\rho \cong 2000$ kg/m3, *$C_s \cong 3300$ m/s,* *$T_{in} = 885.7$ K,* *$P_{th} = -1.887$ GPa*

1. For a perfectly stiff wall, the pressure wave reflects from the wall & returns to the free surf-ace as a pressure pulse

2. $P_{free\text{-}surface} = P_{chamber}$ and the pressure pulse arriving at the free boundary is reflected back as a tensile wave

3. If the net tensile stress > the spall strength, rupture occurs establishing a new surface

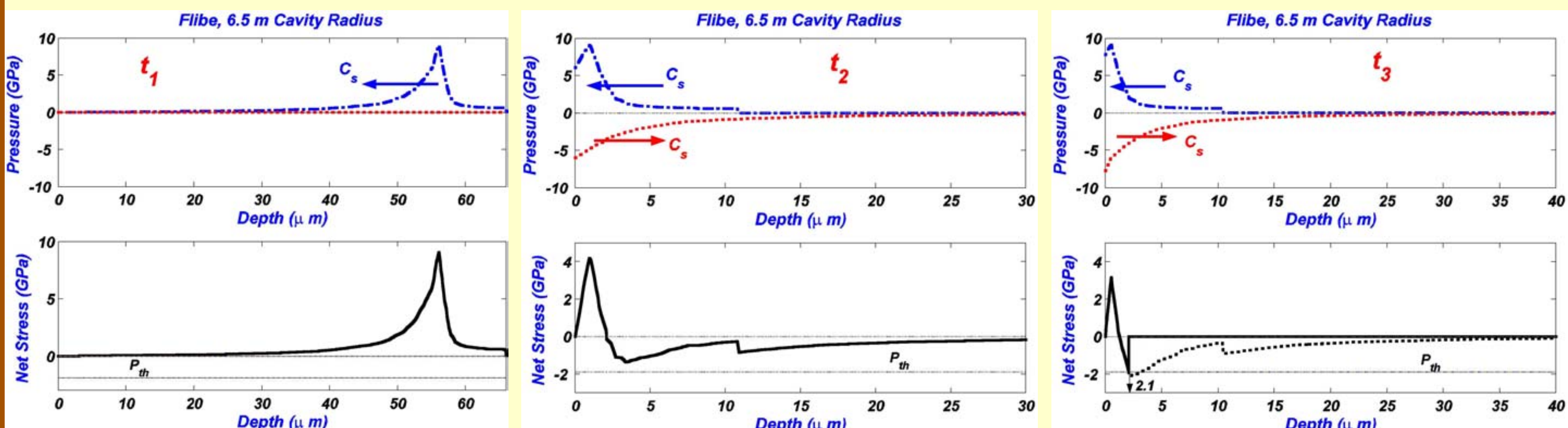

Spalled Thickness $\cong$ 2.1 µm & Spall Time ($t_3 - t_2$) $\cong$ 16.9 ns

Spall time from the beginning of the pressure pulse:
$2\,L/C_s + (t_3 - t_1) \cong 200$ ns for a 0.3 mm flibe layer

Summary of ablation results

		Flibe	Pb
Explosive boiling thickness (µm)	R=0.5 m	**127**	
	R=3.5 m	**10.9**	**3.8**
	R=6.5 m	**4.1**	**2.5**
Spall thickness (µm) (for a wetted wall assuming a perfectly stiff wall except for R=0.5 m which is for a thick free jet case)	R=0.5 m	**28** from free surface at rear of jet	
	R=3.5 m	**4.1**	**1.8**
	R=6.5 m	**2.1**	**1.1**
Total fragmented thickness (µm)	R=3.5 m	**15.0**	**5.6**
	R=6.5 m	**6.2**	**3.6**

Conclusions

- **Residual aerosol can interfere with target and driver injection into the chamber**
- **Several mechanisms exist in liquid-protected IFE chambers to generate aerosol**
- **These mechanisms strongly depend on the details of target emissions and chamber design**
- **Further studies are needed in order to demonstrate acceptable levels of aerosol in a liquid-protected power plant chamber**

Backup

We performed time-resolved measurements of laser plasma expansion and condensation

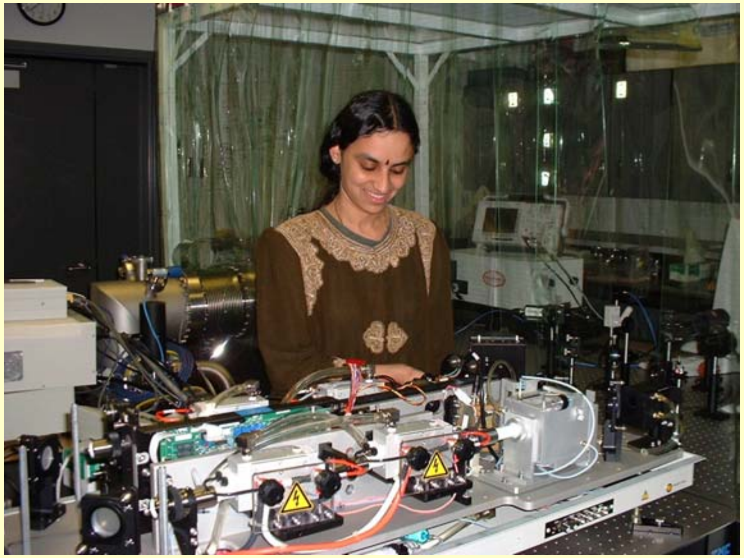

Target : Al, Si
Laser Intensity : 10^7–5×10^9 W/cm^2
Ambient : 10^{-8} – 100 Torr air

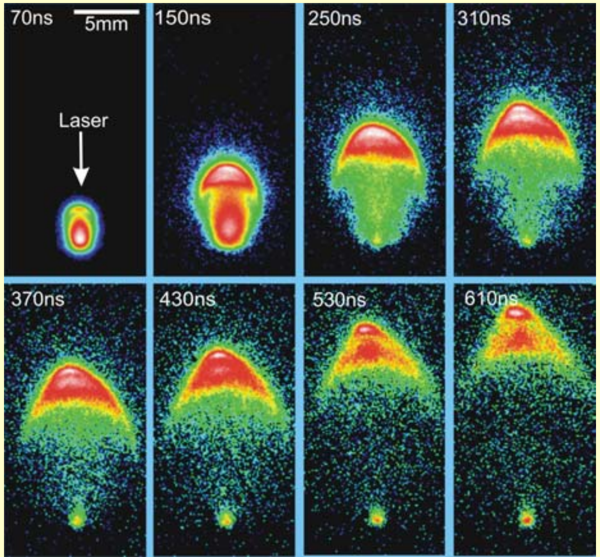

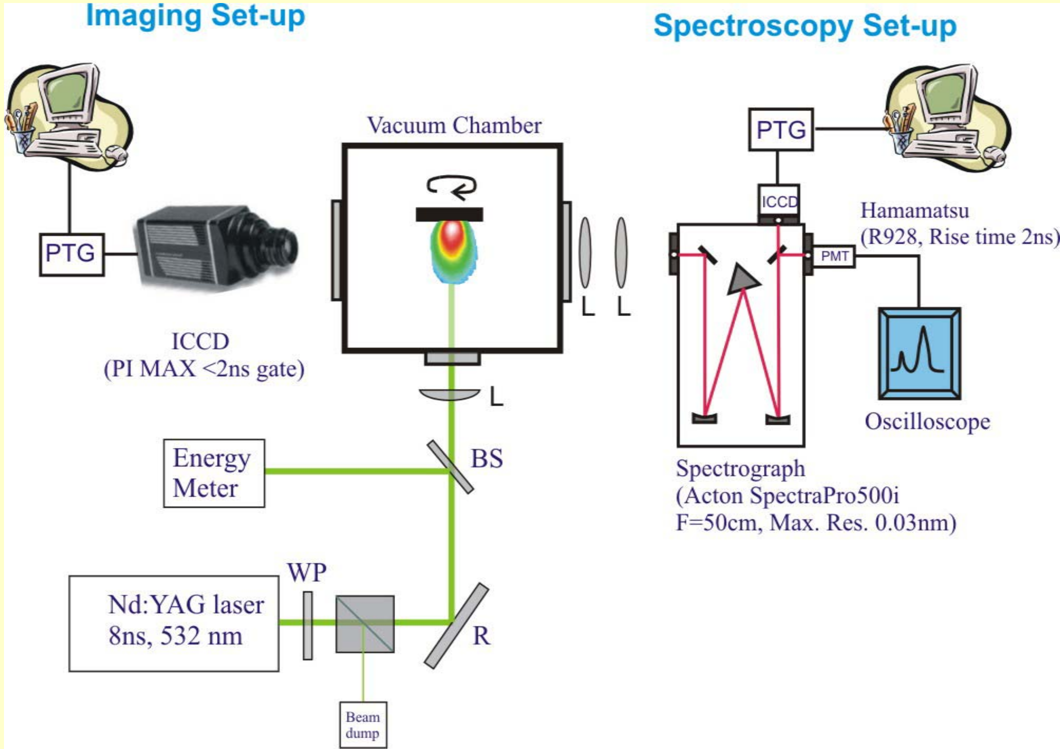

Ionization was shown to dominate condensation in laser ablation plumes

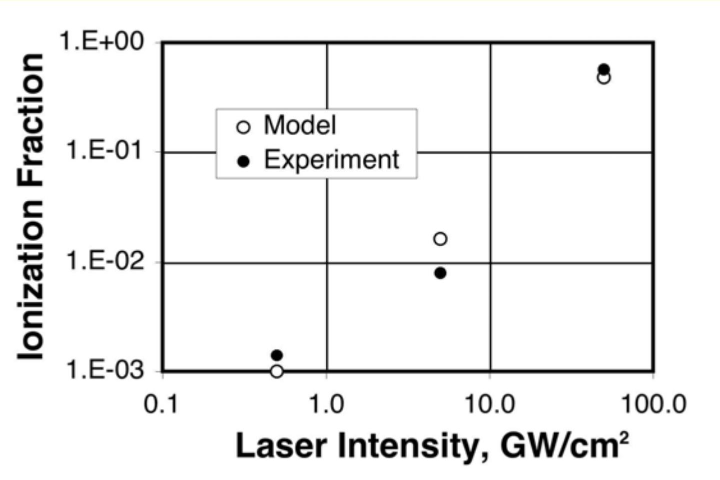

Maximum charge state at 50 ns, 1 mm from Al target, as derived from spectroscopy and assuming LTE.

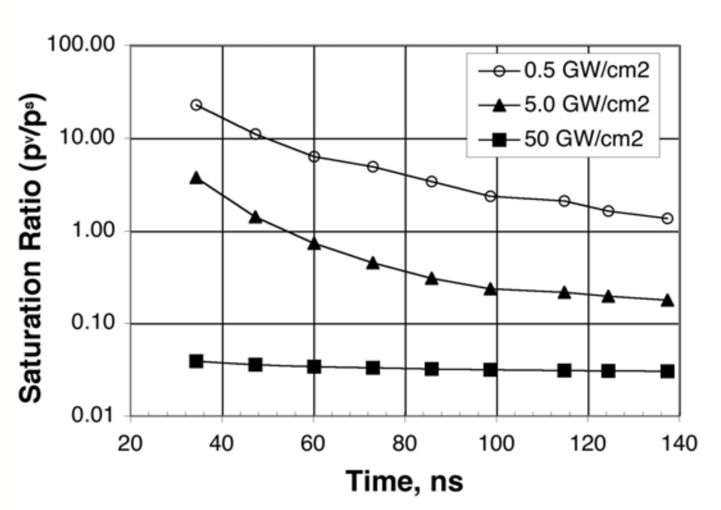

Saturation ratio at 1 mm, derived from spectroscopy and assuming LTE.

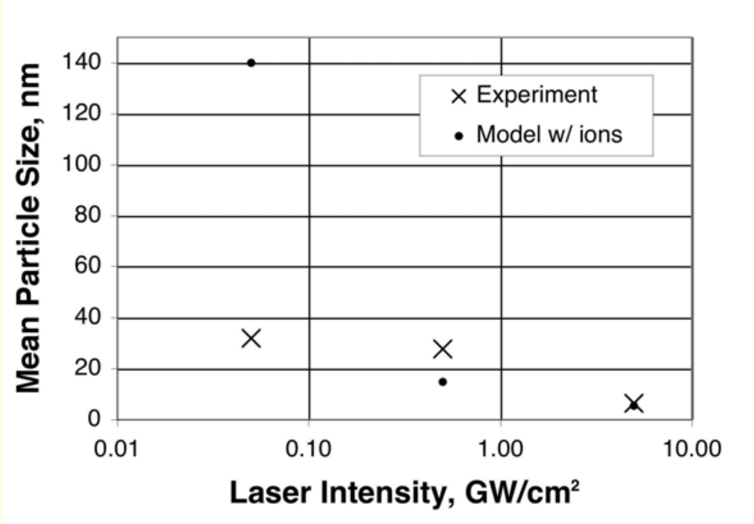

Comparison of experiments and modeling of mean cluster size *vs.* laser intensity.